Combining Asymmetrical Flow Field-Flow Fractionation with Light Scattering and Inductively Coupled Plasma Mass Spectrometric Detection for Characterization of Nanoclay used in Biopolymer Nanocomposites

Bjørn Schmidt, Jens Højslev Petersen, Christian Bender Koch, David Plackett, Nini Johansen, Vimal Katiyar, Erik Huusfeldt Larsen

Combining Asymmetrical Flow Field-Flow Fractionation with Light Scattering and Inductively Coupled Plasma Mass Spectrometric Detection for Characterization of Nanoclay used in Biopolymer Nanocomposites

Journal:	*Food Additives and Contaminants*
Manuscript ID:	TFAC-2008-411.R1
Manuscript Type:	Special Issue
Date Submitted by the Author:	11-Jun-2009
Complete List of Authors:	Schmidt, Bjørn; Technical University of Denmark, National Food Institute; University of Copenhagen, Department of Basic Sciences and Environment Petersen, Jens; Technical University of Denmark, National Food Institute Koch, Christian; University of Copenhagen, Department of Basic Sciences and Environment Plackett, David; Technical University of Denmark, Risø National Laboratory Johansen, Nini; Technical University of Denmark, Risø National Laboratory Katiyar, Vimal; Technical University of Denmark, Risø National Laboratory Larsen, Erik; Technical University of Denmark, National Food Institute
Methods/Techniques:	ICP/MS
Additives/Contaminants:	Food contact materials, Food simulants, Migration, Packaging
Food Types:	

Combining Asymmetrical Flow Field-Flow Fractionation with Light Scattering and Inductively Coupled Plasma Mass Spectrometric Detection for Characterization of Nanoclay used in Biopolymer Nanocomposites

B. Schmidt[a,b], J.H. Petersen[b], C.Bender Koch[a], D. Plackett[c], N. R. Johansen[c], V. Katiyar[c] & E. H. Larsen[b,1]

[a]*Department of Basic Sciences and Environment, University of Copenhagen, Frederiksberg, Denmark;* [b]*The National Food Institute, Technical University of Denmark, Søborg, Denmark;* [c]*Risø National Laboratory for Sustainable Energy, Technical University of Denmark, Roskilde, Denmark*

Abstract

It is expected that biopolymers obtained from renewable resources will in due course become fully competitive with fossil fuel-derived plastics as food packaging materials. In this context, biopolymer nanocomposites are a field of emerging interest since such materials can exhibit improved mechanical and barrier properties and be more suitable for a wider range of food packaging applications. Natural or synthetic clay nanofillers are being investigated for this purpose in a project called NanoPack funded by the Danish Strategic Research Council. In order to detect and chracterize the size of clay nanoparticulates, an analytical system combining asymmetrical flow field-flow fractionation (AF^4) with multi angle light scattering detection (MALS) and inductively coupled plasma mass spectrometry (ICP-MS) is presented here. In a migration study we tested a biopolymer nanocomposite consisting of polylactide (PLA) with 5 % Cloisite®30B (a

[1]E.H Larsen. E-mail: ehlar@food.dtu.dk

derivatised montmorillonite clay) as a filler. Based on AF^4-MALS analyses we found that particles ranging from 50 to 800 nm in radius indeed migrated into the 95 % ethanol used as food simulant. The full hyphenated AF^4-MALS-ICP-MS system showed however, that none of the characteristic clay minerals were detectable, and we conclude that clay nanoparticles were absent in the migrate. Finally, by means of centrifugation experiments, a platelet aspect ratio of 320 was calculated for montmorillonite clay using AF^4-MALS for platelet size measurements.

Keywords: Biopolymer nanocomposites, asymmetrical flow field-flow fractionation, transmission electron microscopy, inductively coupled plasma mass spectrometry, aspect ratio, migration

Introduction

The packaging industry accounts for about 41 % of total global plastic production and out of this 47 % are presently used in food packaging (Fomin and Guzeev 2001). The plastics used for food packaging are at present largely fossil fuel derived. However, polymers obtained from renewable plant resources or biopolymers are now available and are useful in some applications. The sources include fermentation products from agricultural crops and wastes, starch, plant oils, cellulose, gelatine and chitosan. Unfortunately, undesirable biopolymer properties such as brittleness, low thermal stability, and high gas permeability can restrict their practical use. A solution to these problems is to improve the chemical and physical properties of the biopolymer by incorporating nanofillers (Fomin and Guzeev 2001; Ray and Bousmina 2005). Layered aluminium silicates (clays) can be used as nanofillers, but other minerals, such as layered double hydroxides (LDH) (Taviot-Gueho and Leroux 2006) may also be used. Evidently, there is a potential for combining green materials with nanotechnology for the development of a new generation of advanced packaging materials. The overall goal of the on-going NanoPack project (www.nanopack.dk) is to

develop a technological basis for a cost-efficient production and use of biopolymer nanocomposites produced from renewable resources for use in the food packaging industry. These novel nanocomposites must meet the demands made by consumers and various authorities in terms of functionality, sustainability and safety.

Many successful attempts have been made to develop nanocomposite films, and mostly x-ray diffraction and electron microscopy have been used for characterization of the composite structure (Pluta et al. 2002; Pospisil et al. 2004; Rhim et al. 2006; Zhang et al. 2007). Other methods including dielectric spectroscopy (Pluta et al. 2007) and solid state NMR spectroscopy (Bourbigot et al. 2008) have also been explored.

To our knowledge no attempt has been made to characterize materials migrating from nanocomposites into liquid food simulants such as ethanol-water mixtures. The most widely investigated clays for nanocomposites are montmorillonites that have been chemically modified by long hydrocarbon side-chain quaternary ammonium compounds (e.g. Cloisite®, Southern Clay Products, Gonzales, Texas). Depending on the modifier chain length, these clays exhibit more or less hydrophobic surface characteristics. Unfortunately, none of the organomodifiers of this type are yet to be found on the positive list in the current EU food contact plastics legislation (EU 2002). From a food safety point of view it is important to characterize migrates from nanocomposites containing clays as fillers. As a general rule, nanocomposites must comply with the total migration limit of 10 mg dm^{-2} (EU 2002). In order to further characterize nanoparticles contained in such migrates, asymmetrical flow field-flow fractionation (AF^4) is well-suited for determining the size distribution of particles suspended in the food stimulant used for the migration study. In AF^4 an external field force or gradient, rather than partitioning between phases, causes differential retention

of nanoparticles according to their hydrodynamic radius (Giddings 1993). Following the time and size-resolved elution, the analyte particles are carried to one or several detectors. Detection techniques commonly used in conjunction with AF^4 include multi angle light scattering (MALS), or ultraviolet (UV) and fluorescence (FL) spectrometry. In order to acquire data on the sizes (radii) of the separated nanoparticles the MALS detector is particularly useful. This non-destructive detection technique employs a laser beam, which is passed through a flow cell in which the suspended analyte particles cause the incident laser light to be scattered. The intensity of the scattered light is measured simultaneously by several photodiodes placed at different scattering angles in the plane around the cell. By measuring the angular dependence of the scattered light, it is possible to deduce the radius of the particles (Wyatt 1998). The radius of the particles measured by this technique is the so-called root mean square (rms) radius, which is a mass-averaged squared distance of each scattering point in the particle from the particle's center of mass. The theory and application of field-flow fractionation was originally developed by Giddings (Giddings 1966) and is today widely used with MALS detection for particle characterization in environmental analysis. Furthermore, coupling the non destructive technique AF^4-MALS to inductively coupled plasma mass spectrometry (ICP-MS) gives an additional detection and quantisation possibility of a wide range of elements contained in the separated nanoparticles such as nanoclay platelets (Baalousha et al. 2006; Beckett 1990; Hassellöv et al. 1999; Kammer 2005).

The aim of this study was to characterize migrates obtained from PLA nanocomposites with respect to total migration as well as particle size and elemental composition of nanosized matter. For this purpose an analytical platform consisting of AF^4 coupled with MALS and ICP-MS was established and applied. Some of the challenges regarding the correctness of the analytical characterization of

particle size were associated with the high aspect ratio of the nanoclay platelets and the wide size range of these platelets in suspension.

Materials and methods

Chemicals

Sodium dodecyl sulphate (SDS, ReagentPlus ≥98.5 %) and sodium azide (SigmaUltra) were purchased from Sigma-Aldrich (Milwaukee, Wisconsin, USA). Water was obtained from Milli-Q Element water purification system (Millipore, Massachusetts, USA). Ethanol (gradient grade for liquid chromatography ≥99.9 %) and 25 % ammonia solution were obtained from Merck (Darmstadt, Germany). Paraffin oil was obtained from Sigma-Aldrich (Milwaukee, Wisconsin, USA). Glass distilled water was used for the migration study. Nitric acid (PlasmaPURE 67-69 %) and hydrochloric acid (PlasmaPURE 34-37 %) from SCP Science (Champlain, New York, USA) as well as hydrogen peroxide (Suprapur 30 %) and hydrofluoric acid (Suprapur 40 %) from Merck (Darmstadt, Germany) were used for dissolution of the clay minerals.

Clays and polylactide

Two types of Cloisite® clays were used in the experiments, Cloisite®Na^+ and Cloisite®30B. Cloisite®Na^+ is natural montmorillonite clay and Cloisite®30B is montmorillonite, which has been organically modified with methyl tallow bis-2-hydroxyethyl quarternary ammonium cations. The PLA used in this work was L-9000, an L-polylactide obtained from Biomer (Krailling, Germany).

Polylactide and polylactide/Cloisite®30B extrusion

In order to produce films for the migration studies, PLA granulate was first dried under vacuum at 40^{o}C for three hours. Similarly, the Cloisite®30B clay was dried under vacuum at 100^{o}C for three

hours. For practical reasons, PLA and PLA-Cloisite®30B granulates were initially prepared from the starting polymer using a Haake twin-screw extruder with counter-rotating screws. The Cloisite®30B clay were added to the PLA granules at a 5 % w/w loading and physically mixed by mechanical tumbling in a plastic container for five min. In order to ensure adequate adhesion of the clays to the polymer granules, the latter were first mixed with ~0.4 % w/w paraffin oil before clay addition. The twin-screw extruder has four zones and these were typically set to temperatures in the 150-190^{o}C range with increasing temperature from the in-feed to the out-feed. In each case the extrudate was immediately cooled by passing rapidly through a water bath before pelletising. After drying the pellets at 40^{o}C under vacuum for a minimum of three hours, the resulting dried pellets were fed into a Haake single screw extruder with five temperature zones set in the range 150-195^{o}C with increasing temperature from in-feed to out-feed. The extrudate from the single-screw extruder was fed through a film die and then through chill rolls set at 50^{o}C to generate film with thickness in the range of 100-200 µm and width up to 12 cm.

Characterization of polylactide/Cloisite®30B

The nanocomposite used in this study was examined for intercalation and exfoliation of nanoclay platelets in the PLA matrix by x-ray diffraction (XRD) and transmission electron microscopy (TEM).

X-ray diffraction

As shown in equation 1, Bragg's law can be used to calculate the spacing between planes in the lattice of the clays.

$$n \cdot \lambda = 2 \cdot d \cdot \sin\theta \qquad (1)$$

In equation 1, n is an integer , λ is the wavelength of the x-rays, d is the spacing between planes and θ is the angle between the incident x-rays and the scattering planes. Nanocomposite films were studied by x-ray diffraction using a Siemens D500 diffractometer (Bruker, Karlsruhe, Germany) equipped with a Co tube and a diffracted beam monochromator.

Transmission electron microscopy

The morphology of PLA/Cloisite®30B nanocomposites was examined by performing bright field imaging using a Tecnai G^2 transmission electron microscope (FEI Company, Hillsboro, Oregon, USA) optimized for this purpose. The microscope was operated at an accelerating voltage of 200 kV. Ultrathin sections of PLA/Cloisite®30B nanocomposites (~ 80 nm thickness) were prepared at room temperature using a Leica EM UC6 ultramicrotome (Leica Microsystems, Wetzlar ,Germany) equipped with a glass knife. The microtomed slices were transferred directly from a dry glass knife to copper grids for examination in the TEM.

Acid digestion- and inductively coupled plasma mass spectrometry of clays

The two clays were digested according to method 3052 of the United States Environmental Protection Agency (United States Environmental Protection Agency 1996) using a mixture of hydrogen peroxide, nitric-, hydrochloric- and hydrofluoric acids. For determination of elements in the acid-digested clays or in the eluting clay fractions from the AF^4, an Agilent 7500ce ICP-MS system (Agilent Technologies, California, USA), equipped with a Micromist nebulizer, was operated in the non-cell mode. The on-line and real-time coupling of the AF^4-MALS system with the ICP-MS detector was achieved by a short length of capillary tubing from the outlet of the MALS detector to the inlet of the nebuliser of the ICP-MS. The ICP-MS operating conditions used are given in Table 1.

Instrumentation for separation and size determination of clays

Centrifugation

The system consisted of a centrifuge model 3-18K from Sigma Laborzentrifugen (Osterode, Germany) with an 11180 swing bucket rotor. Sample tubes were 15 ml Sarstedt (Nümbrecht, Germany) tubes.

Asymmetrical flow field-flow fractionation with multi angle light scattering detection

The AF^4 instrument used was an Eclipse 3 system equipped with a Dawn HELEOS MALS detector (Wyatt Technology Europe GmbH, Dernbach, Germany), which was used in combination with an Agilent 1200 HPLC system (Agilent Technologies, Santa Clara, California, USA). The AF^4 and MALS operating conditions are given in Table 1.

Migration study

Studies of migration from the biopolymer were carried out in triplicate using a mixture 95 % ethanol and 5 % glass distilled water mixture as a simulant for fatty foods according to the current EU legislation (EU 2002) and European Standard (CEN 2002; 2004). One dm^2 of each of the biopolymer nanocomposite and the pure PLA films were totally immersed into the simulant at 40°C for 10 days. Furthermore, a food simulant blank and food simulant spiked with 2 mg of Cloisite®30B were included in the experiments. One full set of samples were used for gravimetric determination of total migration according to the standardised procedure. Using a second set of samples the migrates were evaporated almost to dryness, re-suspended in 20 ml food simulant and analysed by AF^4-MALS-ICP-MS without any further sample preparation. Prior to analysis the spiked sample was diluted 1:9 with simulant and the analyses were performed using 500 µl injections. The ICP-MS signal intensity of ^{26}Mg was used for on-line detection of clay, due to its high abundance in the clay and at the same time low content in the blank food simulant.

Furthermore, ten millilitres of the same migrates were acid digested and a range of elements characteristic to clay were analysed by ICP-MS for additional characterization of the elemental composition of clay.

Determination of aspect ratio of clay by way of centrifugation

Cloisite®Na^+ (50 mg) was weighed into to each of nine centrifuge tubes and five ml of water and one drop of 25% ammonia solution were added. The ammonia solution was added to enhance the stability of the suspension by electrostatic repulsion of the negatively charged nanoclay platelets at alkaline pH. The suspensions were ultrasonicated for 15 min and mixed overnight attached to a vertical rotating wheel. The next day, the nine solutions were centrifuged at 4700 rpm for two, five, 10, 15, 20, 25, 50, 100 and 200 minutes respectively. From the top one cm, 750 µl supernatant was sampled and 20 µl were injected into the AF^4-MALS for analysis.

Results and discussion

Characterization of biopolymer nanocomposite

PLA/Cloisite®30B structure by wide angle x-ray diffraction

The X-ray diffractogram in Figure 1 (curve B) indicates that Cloisite®30B derivatised with the quaternary ammonium compound had a fairly well-ordered intercalated system with a basal spacing between platelets of approximately 1.8 nm (as indicated at 5.7°2θ) and very little low-angle scattering. In contrast, curve A demonstrates that the PLA/clay nanocomposite was highly disordered with a basal spacing of 1.6 nm (as indicated at 6.3°2θ) and an extensive low-angle scatter from exfoliated plates and PLA.

Transmission electron microscopy

In order to acquire representative TEM images of the nanocomposite, nine images of two nanocomposites were recorded and a representative image is shown in Figure 2. Single exfoliated clay platelets can be observed as needle-shaped bodies in the figure, which suggests that the clay was largely exfoliated in the polymer matrix. Some occurring darker areas also indicated intercalation of clay platelets. The information obtained from the TEM-images therefore confirmed the XRD data, namely that the desired exfoliation of clay indeed occurred in the PLA matrix. This information together with the features of the TEM image also indicated that the individual platelets had large aspect ratios.

Clay analysis using inductively coupled plasma mass spectrometry

Mass spectrometric characterization of elemental composition of clays

The ICP-MS spectra of acid-digested Cloisite®Na^+ shown in Figure 3 A-B were obtained following subtraction of the acid blank from the mass spectrum recorded for the sample. The mass spectrum for Cloisite®30B (data not shown) was similar to that obtained for Cloisite®Na^+. The mass spectrum in Figure 3 showed that Cloisite®Na^+ contained a range of elements that were useful as a multi-variable elemental fingerprint of the clay. In addition to the presence of isotopes of major elements like ^{28}Si, ^{27}Al, ^{58}Fe and ^{26}Mg in the clays, the lower signal intensities of the mass spectra demonstrate that Cloisite®Na^+ also contained a range of trace or ultra-trace isotopes like ^{7}Li, ^{45}Sc, ^{48}Ti, ^{51}V, ^{55}Mn, ^{63}Cu, ^{64}Zn, ^{69}Ga, ^{88}Sr, ^{89}Y, ^{90}Zr, ^{93}Nb, ^{120}Sn, ^{138}Ba, ^{139}La, ^{140}Ce, ^{141}Pr, ^{144}Nd, ^{156}Gd, ^{180}Hf, ^{181}Ta, ^{208}Pb, ^{232}Th and ^{238}U.

Selective on-line detection of clay by inductively coupled mass spectrometry

A fractogram of a nanoclay suspension using the hyphenated AF^4-MALS-ICP-MS system is presented in Figure 4 showing overlaid intensity profiles corresponding to the 90° light scattering

signal and the ICP-MS signals. Isotopes of a minor and a major element, ^{90}Zr and ^{26}Mg, were selected for on-line detection of Cloisite®Na^+ by ICP-MS coupled with AF^4-MALS, because of their low background level or high abundance in the clay matrix, respectively. The fact that the light scattering and ICP-MS signals coincide in time show that particles detected by the MALS detector are in fact clay platelets. Finally, the rms radii derived from the MALS detection show that the platelet radii of the large unresolved AF^4 peak eluting between 10 and 45 min (Figure 4) are in the range 20-250 nm.

Migration study

The results obtained from the migration study in Table 2 report values for total migration, particle sizes of migrated matter, and indicate whether or not clay was detected by ICP-MS in the migrates. Particle sizes of migrated matter were deduced from the cumulative number fraction as depicted in Figure 5 B. The results show that nano-sized particles were detected in the blank food simulant, which suggested that the migration cells or the solvents used as food simulant were contaminated with particles. All total migration values were therefore corrected for this blank value. Furthermore, the standard deviation obtained from the triple gravimetric determinations of all samples was well below the acceptable levels as prescribed in the CEN standard. The migrated substances are thought to be low-molecular weight PLA oligomers from the PLA matrix (Paul et al. 2005; Katiyar Unpublished data) or methyl tallow bis-2-hydroxyethyl quarternary ammonium modifier of the derivatised Cloisite®30B. The results demonstrated (Table 2) that there was a large difference between the pure PLA and the nanocomposite with respect to the particle size distributions and also with respect to the upper particle size limit in the corresponding migrates. Finally, the results of this migration study showed that the amount of total migration differed between the two samples. Both sample materials however, were in compliance with the total migration limit of 10 mg dm^{-2}.

Analysis of the migrate obtained from the nanocomposite material using the full hyphenated analytical system is shown in Figure 6. The fractogram shows that the migrate indeed contained nanosized particulates as indicated by the light scattering signal and that their sizes ranged from 50-800 nm. The 20^{th} to 80^{th} percentiles of the size distribution were 190 nm and 230 nm, respectively, in rms radii as shown in Table 2. The fractogram however, also demonstrates absence of clay as no increase in the time resolved ICP-MS signal was seen for ^{26}Mg within the elution time window. In order to confirm this finding the migrates were separately submitted to acid digestion and the isotope pattern following ICP-MS analysis indeed showed that clay was absent.

Šimon et al. (2008) discussed in theory the possible migration of particles from nanocomposites and concluded that only very small particles with a diameter of about 1 nm could migrate. A prerequisite for this conclusion was that the polymer matrix had a relative low dynamic viscosity and that it did not interact with the nanoparticles. To our knowledge the migration study presented here is the first attempt to characterize migrates from nanocomposites by using size separation and determination by AF^4-MALS-ICP-MS and our results confirm the theoretical predictions by Šimon et al.

Clay aspect ratio

Information on clay aspect ratio, α, was of importance for the correctness of the determination of nanoparticle radius by light scattering techniques. This was mainly because the algorithms applied to the collected raw light scattering data did not immediately apply to estimation of radius of particles with large aspect ratios. The aspect ratio is given by $\alpha = d_{pl}/h$ where h is the thickness and d_{pl} the diameter of the platelet. To prevent large clay platelets from precipitating in the AF^4 channel, removal of this fraction of the suspensions was necessary prior to running the analyses and was

carried out by centrifugation. For a given centrifuge the desired run times in seconds to achieve a certain maximum nanoparticle diameter in the supernatant can be calculated according to Bernhardt (1994)

$$t_s = \ln\left(\frac{r_{out}}{r_{in}}\right)\frac{18\eta}{4\pi^2\Delta\rho d^2\left(rpm/60\right)^2} \quad (2)$$

This equation allows calculation of the time t_s it takes for a spherical particle with a diameter d to travel from a given surface in a tube (fill-up point r_{in}) to a chosen distance below that surface (sampling point r_{out}) at constant force (revolutions per min, rpm). The difference in density of the particles relative to the surrounding medium is given by $\Delta\rho$ and η is the viscosity of the medium. The constant values used in the equation are r_{out} = 12.5 cm, r_{in} = 11.5 cm, $\Delta\rho$ = 1.86 g ml^{-1}, rpm = 4700 and η = 0.000894 Pa s. For non-spherical particles, like nanoclay platelets, equation (2) can not be used. The effective sedimentation diameter d_s for platelets has been described as (Jennings and Parslow 1988):

$$d_s = d_{pl}\sqrt{\frac{1.5}{\alpha}\arctan\alpha} \quad (3)$$

where d_{pl} is the diameter and α is the aspect ratio of a platelet. Combination of equations (2) and (3) yields:

$$t_s = \ln\left(\frac{r_{out}}{r_{in}}\right)\frac{18\eta}{4\pi^2\Delta\rho\left(d_{pl}\sqrt{\frac{1.5}{\alpha}\arctan\alpha}\right)^2(rpm/60)^2} \quad (4)$$

which allows for the estimation of the equivalent travel time for a platelet with diameter d_{pl} and an aspect ratio α.

The two clays included in this study originated from the same montmorillonite source. The determination of α, which was carried out for Cloisite®Na^+ because of its immediate compatibility with aqueous solvents, was based on data obtained from centrifugation tests. The apparent rms radii of the nanoclay platelets in the supernatants obtained following variation of centrifugation time were determined by AF^4-MALS analysis. The 98^{th} percentile of the cumulative number fraction was used to characterize the upper cut-off radius of the size distribution (Figure 5 A). The use of the 98^{th} percentile rather than the maximum value of determined radii improved the robustness of this metric by excluding a few large agglomerated particles from the measured size range.

The experimental fit between centrifugation time and 98^{th} percentile diameter is shown in Figure 7 curve A using 2 times the rms radius from AF^4-MALS as the equivalent diameter, d_{rms}. This value is used as the best estimate of d_{pl} in equation 4. Using d_{rms} as d_{pl} of the platelets we iterate an α value by estimating t_s values which most closely fitted the experimental data. The best fit was obtained by an α value of 320 and can be seen in Figure 7 curve B. The fit obtained using an aspect ratio of 320 however, is valid only for particle sizes (d_{rms}) above 450 nm. This may be due to a different aspect ratio of the fraction of smaller nanoclay platelets but further iterations of the α-value did not lead to any successful match between calculated t_s values and experimental set t_s values for the smaller nanoparticles.

Conclusions

This study demonstrated that AF^4 with MALS detection was useful for characterizing the size of nanoparticles contained in migrates from nanocomposites of PLA and organomodified montmorillonite clay as filler. However, this coupled instrumentation alone did not provide any information on the identity of the nanoparticulates occurring in the food simulant. This limitation was overcome by coupling the AF^4-MALS to the element-selective ICP-MS detector, which provided additional information on trace elements known to be naturally present in the clay. The hyphenated analytical system was used for selective detection and size characterization of suspensions of the unmodified montmorillonite Cloisite®Na^+. Furthermore, the analytical system was applied for characterization of migrates from nanocomposite films of PLA and the organomodified Cloisite®30B montmorrilonite clay used as filler. The results demonstrated that nanoparticulates at 50-800 nm in radius indeed migrated from the nanocomposite but ICP-MS signals corresponding to clay minerals were absent.

A possible drawback to an accurate size determination of nanoclay platelets by the MALS detector is their large aspect ratio. The algorithms of the manufacturer's software for radius calculations of nanoparticles were in theory valid only for specific particle shapes and not for platelets. The experimental determination of the aspect ratio by centrifugation experiments led to a value of about 320, demonstrating a highly anisotropic particle morphology. Applying this aspect ratio made possible a reliable determination of platelet size by AF^4-MALS.

Acknowledgements

The authors would like to thank The Danish Strategic Research Council for funding the NanoPack project. The authors are grateful for assistance on the Tecnai transmission electron microscope provided by personnel at the Center for Electron Nanoscopy, Technical University of Denmark.

References

Baalousha, M, Kammer, FVD, Motelica-Heino, M, Hilal, HS, Le, CP. Size fractionation and characterization of natural colloids by flow-field flow fractionation coupled to multi-angle laser light scattering. 2006. J Chromatogr A. 1104:272-281

Beckett, R. Use of field-flow fractionation to study pollutant-colloid interactions. 1990. J Chromatogr. 517:435-447

Bernhardt, C. Particle size analysis: Classification and sedimentation methods. 1994. Chapman & Hall. London.

Bourbigot, S, Fontaine, G, Bellayer, S, Delobel, R. Processing and nanodispersion: A quantitative approach for polylactide nanocomposite. 2008. Polym Testing. 27:2-10

CEN. 2002. EN 1186: Materials and articles in contact with foodstuffs – plastics. Part 1: Guide to the selection of conditions and test methods for overall migration. Part 14: Test method for

substitute test for overall migration into isooctane and 95% aqueous ethanol. Rue de Stassart 36, Brussels, Belgium

CEN. 2004. EN 13130-1: Materials and articles in contact with foodstuffs – Plastics substances subject to limitation – Part 1: Guide to test methods for the specific migration of substances from plastics to foods and food simulants and the determination of substances in plastics and the selection of conditions of exposure to food simulants, Rue de Stassart 36, Brussels, Belgium.

EU, 2002, Commission Directive of 6 August 2002 relating to plastic materials and articles intended to come into contact with foodstuffs. Official Journal of the European Communities L 220 of 15.8.2002, p. 18, Amendments: 2004/1/EC, 2004/19/EC, 2005/79/EC, 2007/19/EC, 2008/39/EC).

Fomin, VA and Guzeev, VV. Biodegradable polymers, their present state and future prospects. 2001. Prog Rub Plast Technol. 17:186-204

Giddings, JC. A New Separation Concept Based on a Coupling of Concentration and Flow Nonuniformities. 1966. Sep Sci. 1:123-125

Giddings, JC. Field-flow fractionation: analysis of macromolecular, colloidal, and particulate materials. 1993. Science. 260:1456-1465

Hassellöv, M, Lyven, B, Haraldsson, C, Sirinawin, W. Determination of continuous size and trace element distribution of colloidal material in natural water by on-line coupling of flow field-flow fractionation with ICPMS. 1999. Anal Chem. 71:3497-3502

Jennings, BR and Parslow, K. Particle-Size Measurement - the Equivalent Spherical Diameter. 1988. Proc R Soc Lond A Math Phys Eng Sci. 419:137-149

Kammer, FVD. Field-flow fractionation coupled to multi-angle laser light scattering detectors: Applicability and analytical benefits for the analysis of environmental colloids. 2005. Anal Chim Acta. 552:166-174

Paul, M-A, Delcourta, C, Alexandre, M, Dege´e, Ph., Monteverde, F, Dubois Ph. Polylactide/montmorillonite nanocomposites: study of the hydrolytic degradation. 2005. Polym Degrad Stab. 87:535-542

Pluta, M, Galeski, A, Alexandre, M, Paul, MA, Dubois, P. Polylactide/montmorillonite nanocomposites and microcomposites prepared by melt blending: Structure and some physical properties. 2002. J Appl Polym Sci. 86:1497-1506

Pluta, M, Jeszka, JK, Boiteux, G. Polylactide/montmorillonite nanocomposites : Structure, dielectric, viscoelastic and thermal properties. 2007. Eur Polym J. 43:2819-2835

Pospisil, M, Kalendova, A, Capkova, P, Simonik, J, Valaskova, M. Structure analysis of intercalated layer silicates: combination of molecular simulations and experiment. 2004. J Colloid Interface Sci. 277:154-161

Ray, SS and Bousmina, M. Biodegradable polymers and their layered silicate nano composites: In greening the 21st century materials world. 2005. Prog Mat Sci. 50:962-1079

Rhim, JW, Hong, SI, Park, HM, Ng, PKW. Preparation and characterization of chitosan-based nanocomposite films with antimicrobial activity. 2006. J Agric Food Chem. 54:5814-5822

Simon, P, Chaudhry, Q, Bakos, D. Migration of engineered nanoparticles from polymer packaging to food - a physicochemical view. 2008. J Food Nutr Res. 47:105-113

Taviot-Gueho, C and Leroux, F. In situ polymerization and intercalation of polymers in layered double hydroxides. 2006. Struct Bond. 119:121-159

United States Environmental Protection Agency. Method 3052 - Microwave assisted acid digestion of siliceous and organically based matrices. 1996. United States Environmental Protection Agency. 1-20

Wyatt, PJ. Submicrometer particle sizing by multiangle light scattering following fractionation. 1998. J Colloid Interface Sci. 197:9-20

Zhang, XQ, Do, MD, Dean, K, Hoobin, P, Burgar, IM. Wheat-gluten-based natural polymer nanoparticle composites. 2007. Biomacromolecules. 8:345-353

Figure 1. X-ray diffraction patterns of, A, PLA containing 5 % Cloisite®30B and B, pure Cloisite®30B.

Figure 2. TEM micrograph of a biopolymer nanocomposite consisting of PLA with 5 % Cloisite®30B and paraffin oil as wetting agent.

Figure 3. Mass spectra of Cloisite®Na^+. The spectra have been divided into two. A, signal intensity between 5000 and 1000000 and B, above 1000000. The clays were dissolved in acid according to the procedure described in the experimental section.

Figure 4. AF^4-MALS-ICP-MS detection of nanoclay in the supernatant of a suspension of 50 mg Cloisite® Na^+ in 5 ml water following centrifugation for 50 minutes at 4700 rpm. The four curves represent a main constituent (^{26}Mg, left y-axis), a trace constituent (^{90}Zr, right y-axis), the 90° light scattering signal intensity (right y-axis, relative signal to be multiplied by 900) and rms radius (right y-axis) as a function of retention time.

Figure 5. Evaluation of the cumulative number fraction curves from suspensions of nanoclays. (A) Supernatant following centrifugation for 10 minutes of Cloisite®Na^+ and (B) Food simulant spiked with Cloisite®30B. Particle sizes are given as root mean square (rms) radius.

Figure 6. Combined AF^4-MALS and ICP-MS data for a migrate from PLA containing 5 % Cloisite®30B.

Figure 7. Nanoparticle diameter as a function of centrifugation time and. The curves represent, A, Experimental d_{rms} determinations of Cloisite®Na^+ in supernatants as a function of centrifugation times, B, d_s as a function of modelled centrifugation times applying d_{rms} as d_{pl} and an aspect ratio of 320 in calculations of d_s.

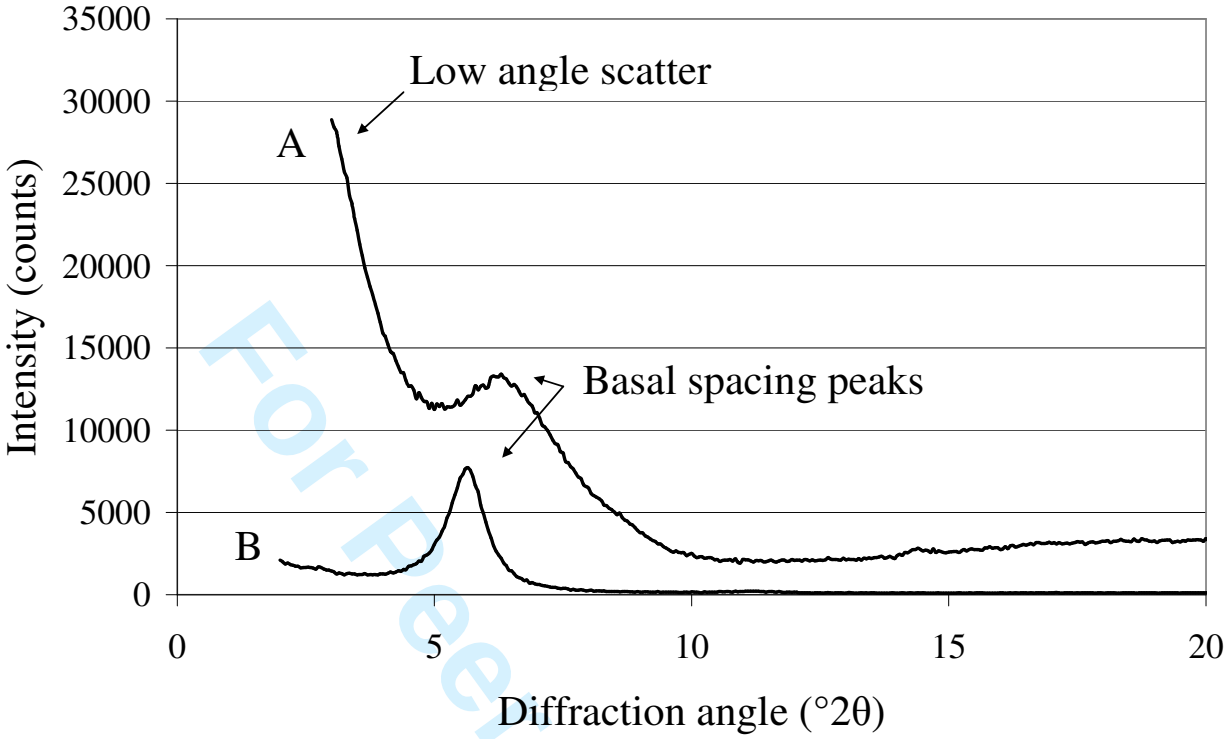

Figure 1.

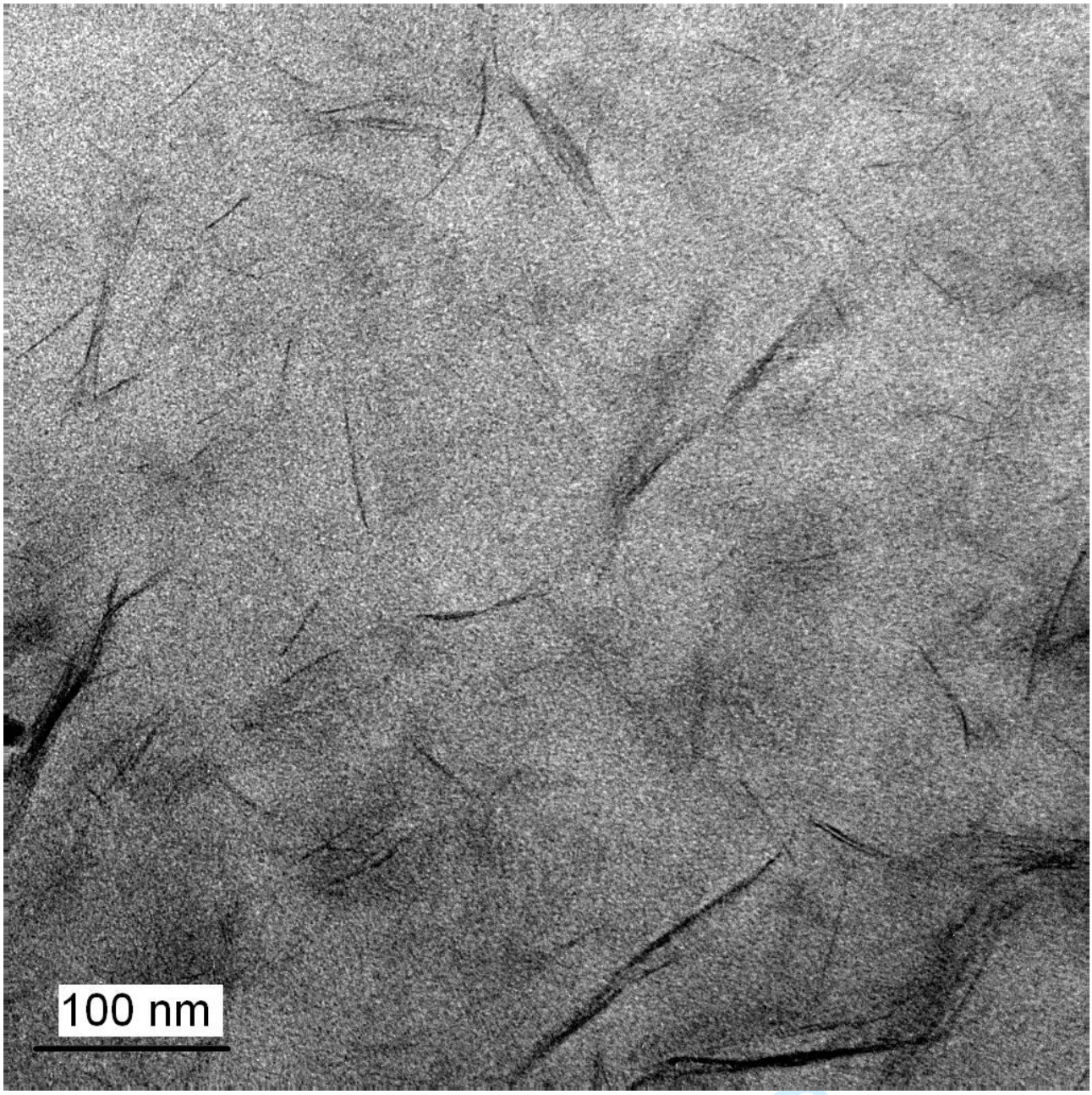

Figure 2.

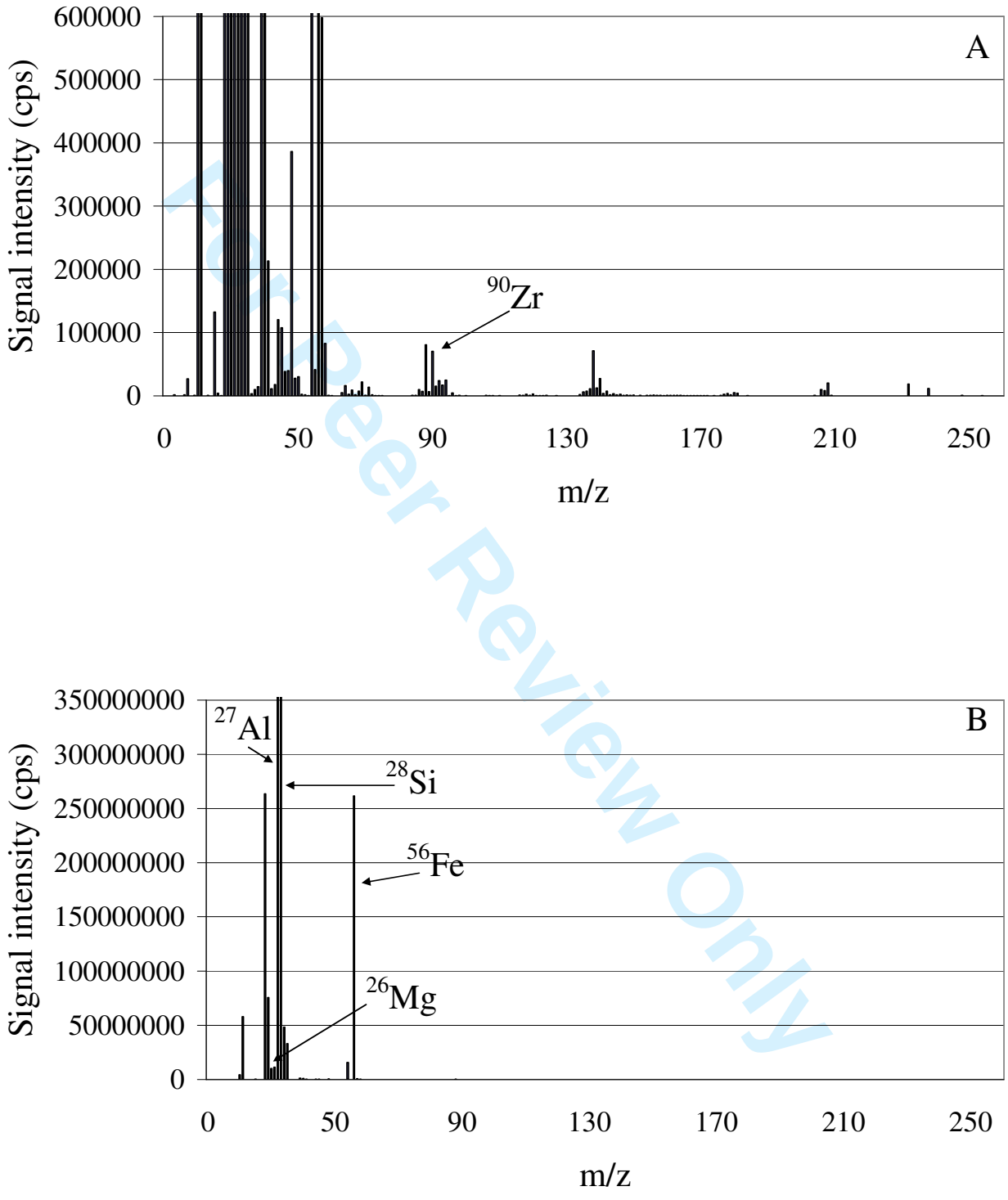

Figure 3.

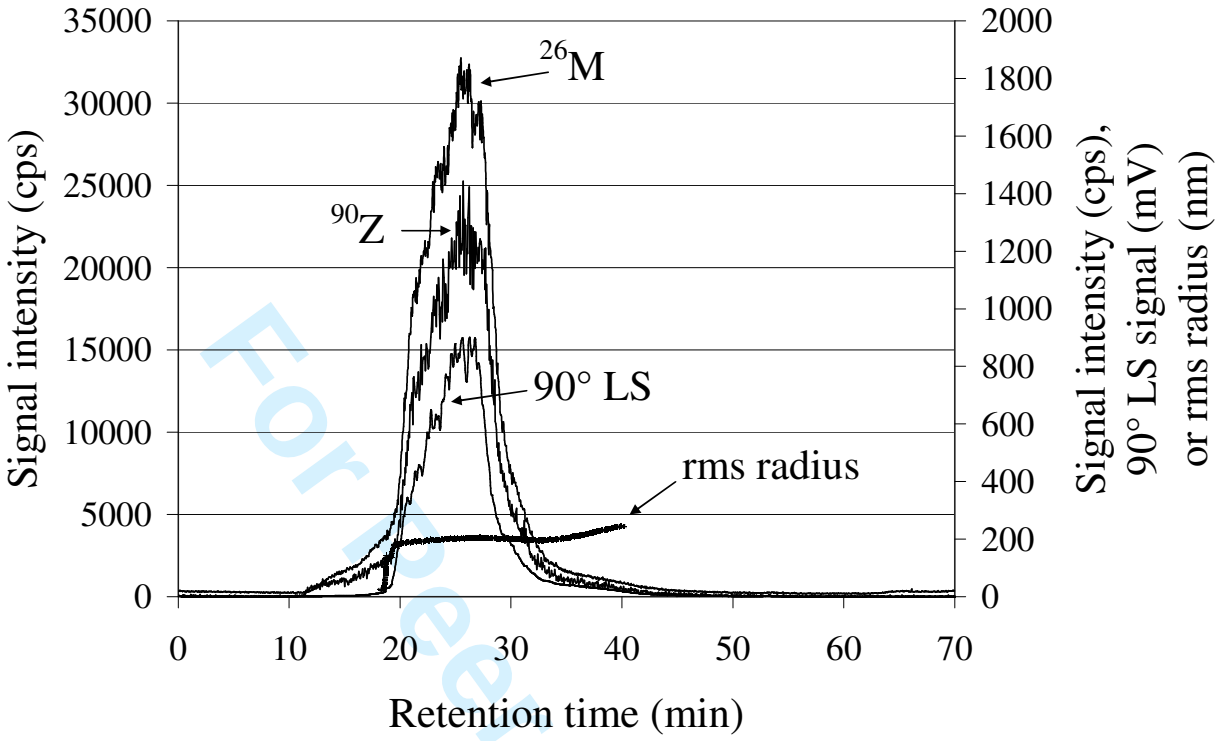

Figure 4.

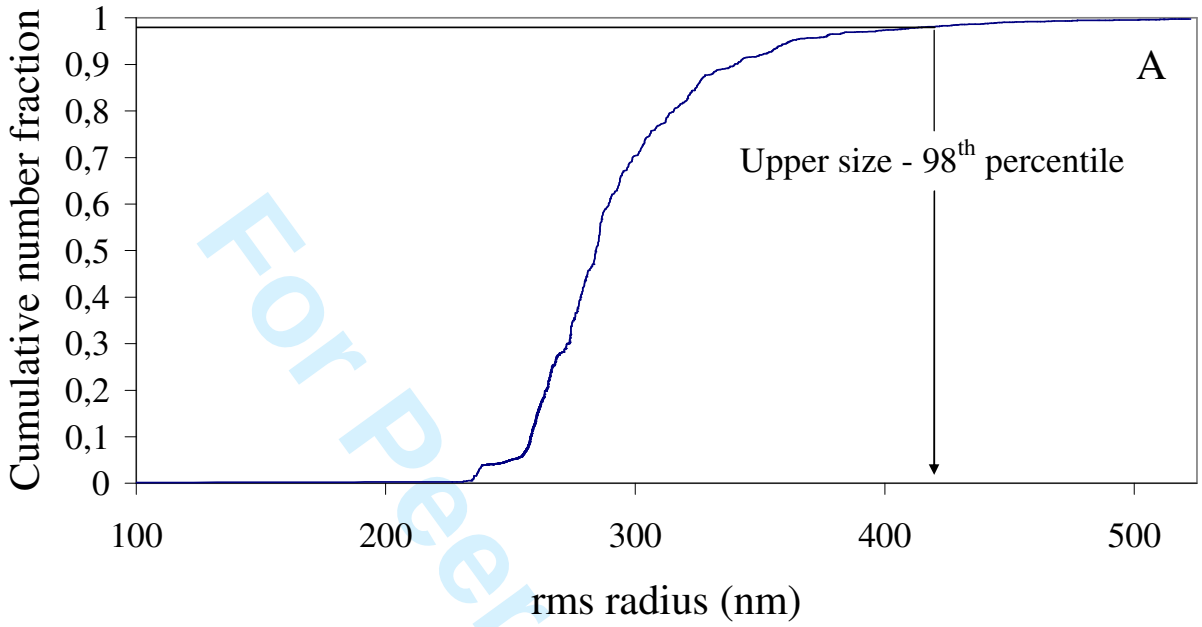

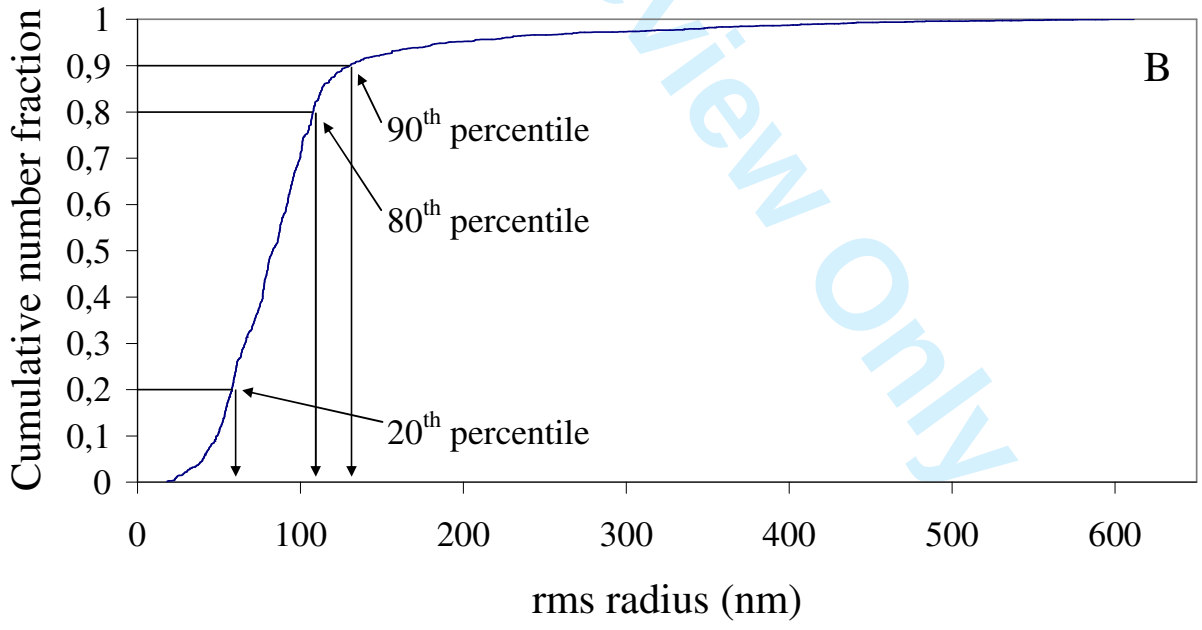

Figure 5.

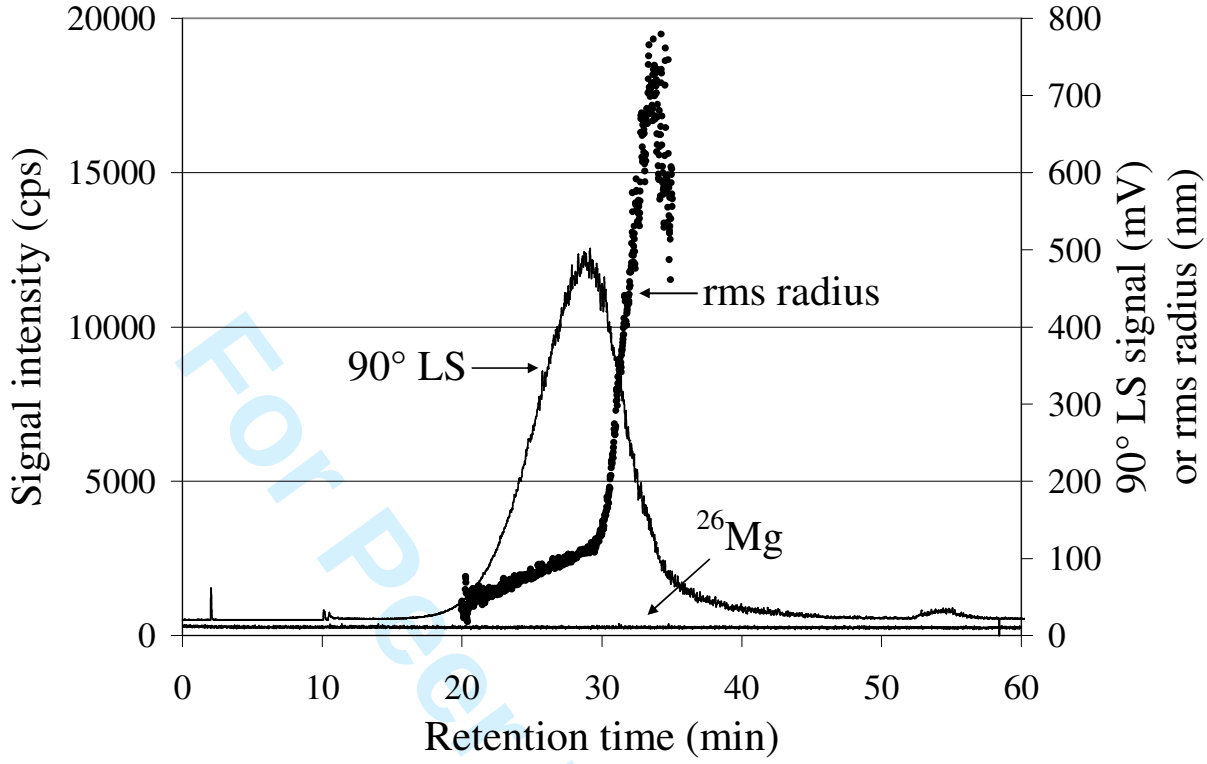

Figure 6.

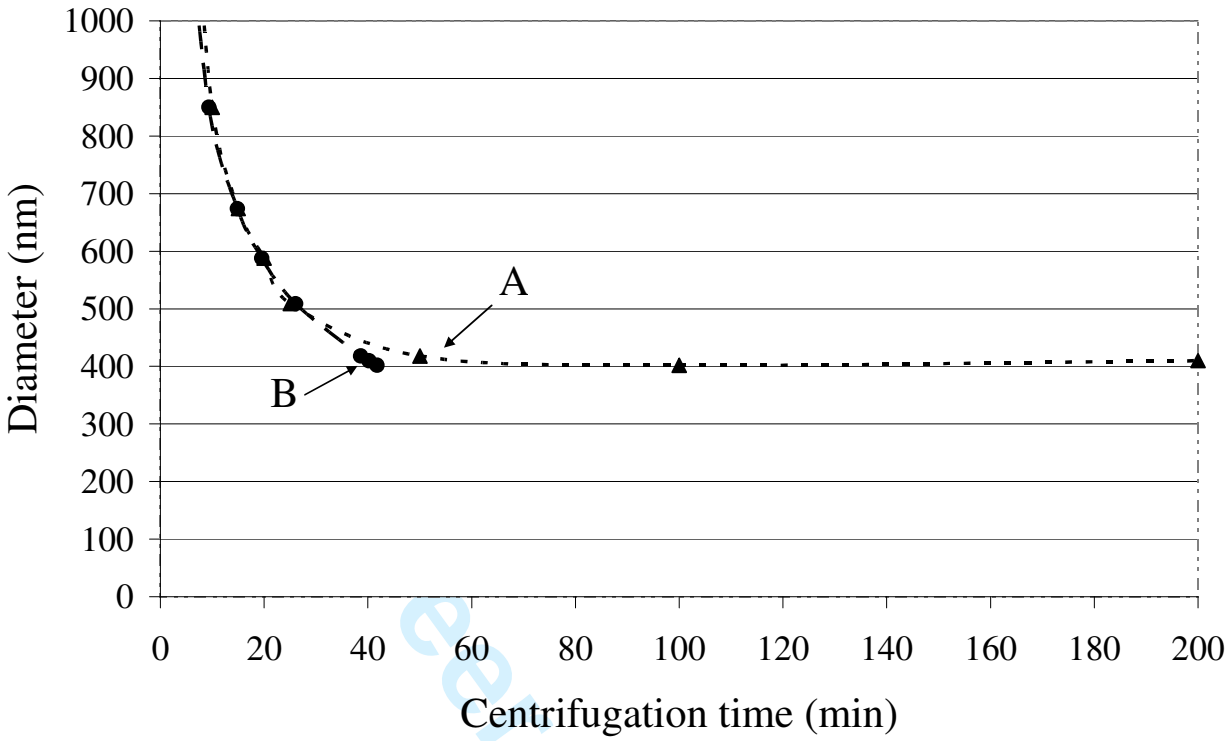

Figure 7.

Table 1. Operating conditions for the AF^4-MALS and the ICP-MS

AF^4-MALS operating conditions					
Channel	Short channel with a "wide" 350 µm thick spacer and a 10 kDa pore size regenerated cellulose membrane				
Carrier	0.05% SDS and 200 ppm sodium azide in water				
Fitting algorithm	Berry 2nd order polynomial fit				
Collection interval	1 second				
Flow Field-flow fractionation program					
Time (min)	Detector Flow (ml min^{-1})	Cross Flow (ml min^{-1})	Focus Flow (ml min^{-1})	Injection Flow (ml min^{-1})	Mode
0-2	1	0.5	0	0	Elution
2-3	1	-	2	0	Focus
3-9	1	-	2	0.2	Focus+Injection
9-10	1	-	2	0	Focus
10-30	1	0.5-0.1 linear gradient	0	0	Elution
30-52	1	0.1	0	0	Elution
52-61	1	0	0	0	Elution
61-70	1	0	0	0.2	Elution+Injection

ICP-MS operating conditions		
	Mass scan m/z 6-254	Time resolved detection of m/z 26 and 90
RF power	1500 W	1550 W
Carrier gas	0.83 L min^{-1}	0.88 L min^{-1}
Makeup gas	0.33 L min^{-1}	0.31 L min^{-1}
Number of points per mass	3	1
Acquisition time	111 s	4198 s
Number of repetitions	1	1

Table 2. Results from the migration studies

Parameter measured				
Sample	Total migration (mg dm^{-2})	rms radius range corresponding to 20^{th}-80^{th} percentile[b] (nm)	rms radius corresponding to 90^{th} percentile[b] (nm)	Cloisite®30B detected in migrates by ICP-MS after acid digestion[c]
Blank simulant	0.4	20-31	40	No
Pure PLA	1.7[a] ± 0.6	20-40	100	No
PLA/5% Cloisite®30B	6.7[a] ± 0.5	190-230	235	No
Spiked simulant	2.1[a] ± 0.5	60-110	130	Yes

[a]Values are corrected for the blank simulant
[b]Percentiles are given for the size distribution of measured radius of nanoparticulates
[c]Based on signal intensities of ^{26}Mg being significantly higher blank